Structure
Article

EcxAB Is a Founding Member of a New Family of Metalloprotease AB_5 Toxins with a Hybrid Cholera-like B Subunit

Natasha M. Ng,[1,4] Dene R. Littler,[1,4] Adrienne W. Paton,[2] Jérôme Le Nours,[1] Jamie Rossjohn,[1,3] James C. Paton,[2] and Travis Beddoe[1,*]
[1]ARC Centre of Excellence in Structural and Functional Microbial Genomics, Department of Biochemistry and Molecular Biology, School of Biomedical Sciences, Monash University, Clayton, VIC 3800, Australia
[2]Research Centre for Infectious Diseases, School of Molecular and Biomedical Science, University of Adelaide, SA 5005, Australia
[3]Institute of Infection and Immunity, School of Medicine, Cardiff University, Heath Park, Cardiff CF14 4XN, UK
[4]These authors contributed equally to this work
*Correspondence: travis.beddoe@monash.edu
http://dx.doi.org/10.1016/j.str.2013.08.024

SUMMARY

AB_5 toxins are composed of an enzymatic A subunit that disrupts cellular function associated with a pentameric B subunit required for host cell invasion. EcxAB is an AB_5 toxin isolated from clinical strains of *Escherichia coli* classified as part of the cholera family due to B subunit homology. Cholera-group toxins have catalytic ADP-ribosyltransferases as their A subunits, so it was surprising that EcxA did not. We confirmed that EcxAB self-associates as a functional toxin and obtained its structure. EcxAB is a prototypical member of a hybrid AB_5 toxin family containing metzincin-type metalloproteases as their active A subunit paired to a cholera-like B subunit. Furthermore, EcxA is distinct from previously characterized proteases and thus founds an AB_5-associated metzincin family that we term the toxilysins. EcxAB provides the first observation of conserved B subunit usage across different AB_5 toxin families and provides evidence that the intersubunit interface of these toxins is far more permissive than previously supposed.

INTRODUCTION

AB_5 toxins are key virulence factors produced by a range of pathogenic bacteria known to be the causative agents of diseases such as cholera, whooping cough, and dysentery. Each AB_5 protein consists of two components: a pentameric B subunit that targets eukaryotic cells by binding to glycans located at the cell surface and a catalytic A subunit that disrupts host cellular function following internalization. Different families of AB_5 toxins have been categorized according to the level of sequence conservation in the A and B subunits as well as the A subunit's enzymatic activity. Four families are currently known: the Shiga toxins inhibit protein synthesis using a ricin-like catalytic subunit (Fraser et al., 1994), the pertussis and cholera toxin groups carry unrelated ADP-ribosyltransferases, and SubAB cytotoxin acts as a subtilase-like serine protease (Beddoe et al., 2010). The B subunits of each family share structural, but not sequence, homology, while the A subunits are only related within a family (Merritt and Hol, 1995). Despite structural conservation among their B subunits, each AB_5 protein targets its own cell subpopulations, as minor binding site differences can drastically alter host receptor specificity (Merritt et al., 1997). Moreover, multiple ligand binding sites within the B subunit can also serve to broaden the target cell specificity (Holmner et al., 2007, 2011). Additional complexity is also present within the pertussis toxin whose B subunit gene has expanded and diverged, resulting in an atypical heteropentamer (Stein et al., 1994), so despite the similarities inherent in these toxins, the underlying mechanisms of host cell recognition and disruption can be disease specific.

The pathway of cellular disruption by the cholera AB_5 protein has been well defined and stands as a canonical mechanism of AB_5 action (De Haan and Hirst, 2004). The toxin's B subunit orchestrates the initial stages of this complex invasive process. Briefly, each B subunit within the pentamer can bind glycolipid headgroups such as those of monosialotetrahexosylganglioside (GM_1) at the plasma membrane instigating endocytosis and migration of the holotoxin through the *trans*-Golgi network to the endoplasmic reticulum (ER) via retrograde trafficking. The A subunit then undergoes proteolytic cleavage into two disulfide-linked sections: a larger enzymatic A1 domain and an A2 domain interfaced with the B5 pentamer. Finally, this disulfide link is actively reduced, permitting A1 domain dissociation and its retrotranslocation to the cytosol where its ADP-ribosyltransferase activity corrupts regulation of fluid secretion.

The cholera-like toxins are the largest subgroup of AB_5 proteins including both the archetype cholera toxin (Ctx) and related heat-labile enterotoxins (LT-I and LT-II). Genes encoding two novel cholera-family B subunits were identified and characterized within clinical isolates of *Citrobacter freundii* and *Escherichia coli* derived from diarrheal patients (Karasawa et al., 2002). These new toxin B subunits were, respectively, named CfxB and EcxB. When the structure of CfxB was solved, it confirmed the placement of these proteins within the cholera group (Jansson et al., 2010). The B subunits of all previously studied toxins from the cholera group pair with a related series of A subunits, a conserved family of ADP-ribosyltransferases. In contrast, the genes for CfxB and EcxB are located

Table 1. Data Collection, Processing, and Refinement Statistics

Statistics[b]	Apo EcxAB	GM1:EcxAB
Resolution limits (Å)[a]	39.5–1.86 (1.9–1.86)	34.3–1.80 (1.9–1.80)
X-ray wavelength (Å)	0.9537	0.9537
Space group	$P6_522$	$P6_522$
Unit-cell parameters (Å)	120.7, 120.7, 274.3	120.4, 120.4, 273.4
No. of observations[a]	1,157,466 (169,463)	790,884 (102,891)
No. of unique reflections[a]	992,067 (14,280)	107,527 (15,448)
Mosaicity	0.7	0.4
Completeness (%)[a]	99.9 (100)	99.5 (99.5)
Multiplicity	11.9	7.4 (6.7)
$R_{p.i.m.}$ (%)[a,b]	6.2 (46.7)	4.3 (38.8)
$<I/\sigma(I)>$[a]	9.2 (1.6)	11.7 (2.0)
R factor (%)[c]	17.5	17.8
R-free (%)[d]	20.8	19.8
Isotropic B factor (Zn)	37.2 (43.9)	37.6 (41.5)
Number of atoms		
Protein	6159	6169
Water (Zn)	608 (1)	573(1)
GM1	n/a	340
rmsd bonds (Å)	0.007	0.007
rmsd angles (°)	1.1	1.1
MOLPROBITY results (%)		
Ramachandran favored	99.7	99.7
Ramachandran outliers	0.3 (Gly-281)	0.3 (Gly-281)

[a]Values in parentheses refer to the highest resolution bin.
[b]$R_{p.i.m.} = \Sigma_{(hkl)} [1/(N-1)]^{1/2} \Sigma_i | I_{i(hkl)} - < I_{(hkl)} > | / \Sigma_{(hkl)} \Sigma_i < I_{(hkl)} >$ where N is the redundancy of the *hkl* reflection.
[c]$R_{factor} = (\Sigma | |F_o| - |F_c| |) / (\Sigma |F_o|)$ - for all data except as indicated in footnote d.
[d]Five percent of data were used for the R_{free} calculation (see footnote c).

downstream of their respective *cfxA* and *ecxA* genes, neither of which encode proteins with homology to any previously studied AB_5 protein (Jansson et al., 2010; Karasawa et al., 2002). Instead, the A subunits aligned with a group of uncharacterized bacterial proteins with weak homology to zinc-dependent metzincin metalloproteinases (Jansson et al., 2010) (20%–25% sequence identity to human matrix metalloproteinase 2 [MMP2]).

In the present study, we have determined the X-ray crystal structure of the entire EcxAB holotoxin to 1.86 Å resolution in both apo- and receptor-bound forms. We confirm that EcxA and EcxB pair together and thus represent a member of the AB_5 toxin superfamily. Furthermore, we demonstrate that EcxA is an endopeptidase that stands as a founding member of a family of metzincin metalloproteases, that of the toxilysins, deserving further characterization. Intriguingly, this EcxA subunit docks with its cholera-like EcxB pentamer through an A2 domain, involving a redox-switching 3_{10} helix. EcxAB and CfxAB thus represent founding members of a unique AB_5 family hybrid that comprises B subunits very similar to that of cholera toxin but pair through an entirely different mechanism to an unrelated catalytic A subunit. The EcxAB structure presented here demonstrates a significant level of binding plasticity within cholera-like toxin B subunits. Such binding plasticity may allow a plethora of possible A2 domains to bind, increasing AB_5 toxin evolvability, possibly having implications for the time frames over which pathogenic bacteria and their bacteriophages have been or are able to adapt.

RESULTS

EcxAB, a Novel AB_5 Toxin

The Ecx and Cfx operon structures contain conserved cholera toxin-like B subunit genes (Jansson et al., 2010) downstream of novel A subunit genes (Karasawa et al., 2002). EcxA and CfxA share 78% sequence identity to each other but are not related to ADP-ribosyltransferases such as CtxA or, indeed, any known AB_5 toxin subunit. Instead, they contain a HExGHxxGxxH motif characteristic of the metzincin family of metalloproteases (Tallant et al., 2010) but only 10–20 conserved residues outside this sequence. We have recently shown that coexpression of EcxA and EcxB results in the formation of a stable heterohexameric protein complex (Ng et al., 2013), confirming that EcxAB represents an AB_5 toxin. To ascertain whether EcxA truly was a metalloprotease as well as understanding the nature of the EcxAB holotoxin's intersubunit interaction mechanism, we sought to determine its structure. Following optimization, crystals of the purified EcxAB holotoxin could be grown that diffracted to 1.86 Å resolution. An initial model was obtained using CtxB (Merritt et al., 1997) as a molecular replacement model, yielding clear electron density for the remaining A subunit that allowed it to be built (see Experimental Procedures and Table 1 for details). The final model is largely complete (residues 20–267 and 20–118 for EcxA and B subunits), with only two breaks in electron density corresponding to flexible loops within the A subunit (residues 68–71 and 103–107). The EcxAB crystals contain a single heterohexameric AB_5 complex in the asymmetric unit (63% solvent). The structure has a global organization similar to other AB_5 toxins (Figure 1), with EcxB adopting a homopentameric ring-shaped assembly. The unique Ecx A subunit is composed of two domains, A1 and A2, linked together via a disulfide bond between residues Cys-208 and Cys-271. Similar, but not structurally homologous, A1-A2 linking disulfides are found in other AB_5 toxins. The C-terminal A2 domain contains an eight-amino-acid 3_{10} helix that penetrates into the central pore of the B subunit (Figures 2B and 3).

The Cholera-like EcxB Pentamer

Each monomer of EcxB possesses six antiparallel β strands and two α helices forming an oligonucleotide and oligosaccharide binding fold (OB fold). As in other cholera-family toxins, helix 1 is anchored to β strand 5 via a disulfide bond (Cys-9 to Cys-86) (Jansson et al., 2010; Merritt et al., 1995; van den Akker et al., 1996). There are five copies of EcxB within the asymmetric unit that, despite being under the influence of different packing constraints, are essentially identical. We label the five EcxB monomers $EcxB_1$ to B_5, and they homooligomerize to form a typical AB_5-pentameric ring (see Figure 1B). The structure of each EcxB monomer and its orientation within this pentameric

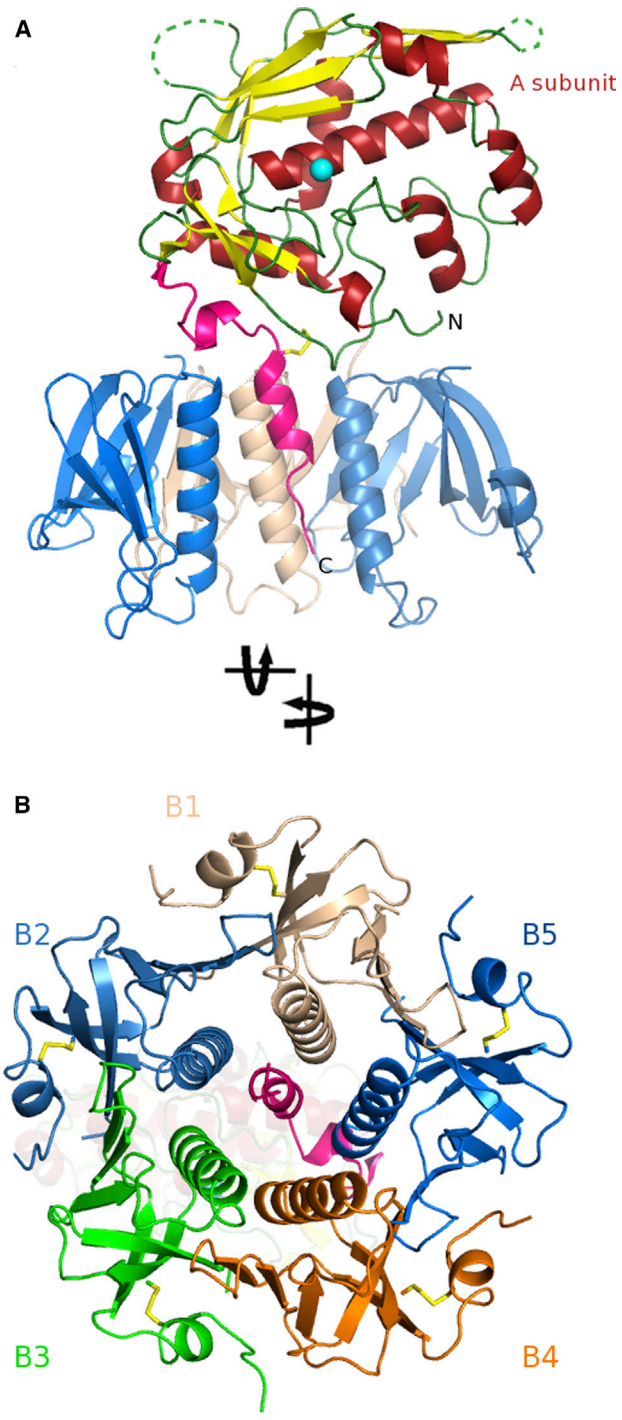

Figure 1. Overall Structure of the EcxAB Holotoxin

(A) Displays the global organization of the EcxAB holotoxin in a cartoon representation. For EcxA, secondary structural elements are labeled and colored with helices in red and β strands in yellow. The A2 segment is highlighted in pink, with the A1-linking disulfide also shown. Three of the five EcxB subunits are colored in blue, tan, and light blue. $EcxB_3$ and B_4 are not displayed in this orientation. Dotted green lines represent loop regions unable to be built into electron density. (B) The organization of the EcxAB pentamer is seen clearly from beneath the molecule utilizing the same coloring as in Figure 2A. $EcxB_3$ and B_4 are shown in green and orange.

See also Figure S1 and 3D Molecular Model S1.

assembly are almost identical to those of other cholera family toxins. The closest structural homologs are CfxB (86% sequence identity, root-mean-square deviation [rmsd] of 0.8 Å over 451 C_α) (Jansson et al., 2010), CtxB (63% sequence identity, rmsd of 0.5 Å over 515 C_α) (Merritt et al., 1997), and the heat-labile toxin B subunits (66% sequence identity, 0.5 Å over 518 C_α with LT-IIb) (van den Akker et al., 1996; see Figure 1 and Figure S1 available online).

Glycan Binding by EcxB

To gain access to host cells, AB_5 toxins bind glycan receptors on the host surface via the B pentamer. The residues making up the cholera toxin's ganglioside GM_1 (Galβ3GalNAcβ4(NeuAcα3)Galβ4Glcβ1Cer) binding site are largely identical in EcxB, suggesting a conserved mechanism of cell targeting. Accordingly, we sought to understand the receptor specificity of EcxB via glycan array analysis performed at the Consortium of Functional Glycomics (CFG). EcxB showed a high degree of binding specificity for the glycan moiety of ganglioside GM_1 (Galβ3GalNAcβ4(NeuAcα3)Galβ4Glcβ1Cer) and its fucosylated derivatives but very little binding to other glycans (Table 2). This is not surprising, as the close homologs CtxB and CfxB also bind GM_1. CfxB had previously been shown to have an affinity for neolacto-(Galβ4GlcNAcβ-) and blood group A type 2-(GalNAcα3(Fucα2)Galβ4GlcNAc) terminated glycans (Jansson et al., 2010). EcxB showed no affinity for these glycans, suggesting a more cholera-like glycan-binding site. To ascertain whether this was the case, we transferred EcxAB crystals into a solution containing the GM_1 pentasaccharide head group prior to freezing, after which a 1.86 Å data set was collected (see Table 1 for data collection and refinement statistics). The overall structure of EcxAB is largely unchanged by GM_1 binding; those sections of EcxA furthest away from EcxB are not as well defined as in the unliganded structure. Correspondingly, the s4 s5 loop; the s7, s8, and s9 β sheet; and helix 4 have higher B factors following refinement. In contrast the remainder of EcxA and the B pentamer are clearly visible with calculated omit maps showing good density for GM_1 in all five B subunit binding sites (see Figure 4A). Electron density is clear for each sugar moiety in all sites, allowing five independent copies of the ligand to be built and their interactions to be defined with a high degree of confidence.

The glycan binding site of EcxB is largely equivalent to that of CtxB; all residues forming direct hydrogen bonds with GM_1 are conserved (see Figures 4A and 4B). The similarities of the glycan binding sites in EcxAB and CtxAB suggest that they target similar cellular subtypes. Comparisons made between cholera and heat-labile toxins have shown that minor differences within the glycan binding sites nevertheless leads to substantial effects on specificity (Holmner et al., 2011); the affinity of EcxAB for GM_1 was thus determined by surface plasmon resonance (SPR) (Figure 4C). A kinetic analysis of EcxAB binding as measured by SPR could not be modeled with an appropriate fit due to the multivalent nature of the EcxB pentamer. However, an apparent K_D was determined by pseudoequilibrium analysis, a method used for other AB_5 toxins in previous publications. The apparent dissociation constant, K_D, of EcxAB for binding to GM_1 is 32 ± 2 nM, and as expected, given the level of sequence identity within their binding sites, is similar to that published for CfxB

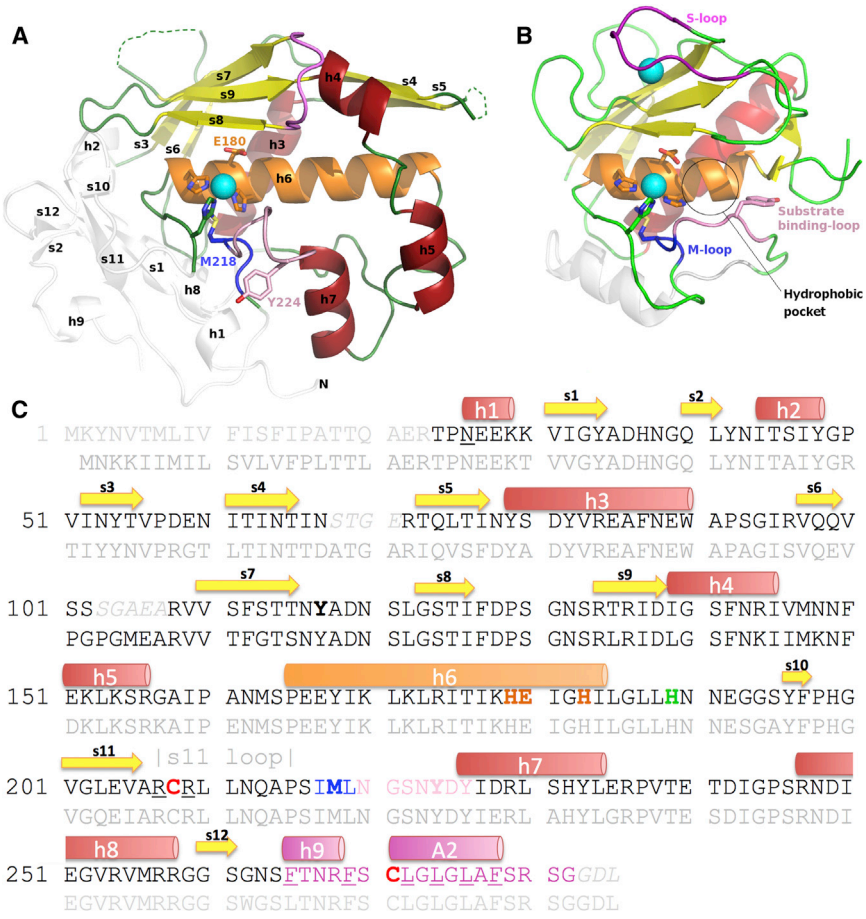

Figure 2. The EcxA Endopeptidase Domain and Its Comparison with MMP2

(A) The structure of the catalytic sections of the EcxA subunit is shown highlighting the bound zinc ion and proteolytic active site. Secondary structural elements are labeled and colored with helices in red and β strands in yellow. The metzincin NTD module is deemphasized by being displayed as partially transparent.

(B) For comparison, an identical alignment of the catalytic CTD module of the human matrix metalloprotease 2 is shown. Colored sections highlight the catalytically important residues discussed in text and are labeled and colored accordingly (PDB ID 1EAK).

(C) Sequence of EcxA shown above that of CfxA; the extent of the various secondary structure elements are depicted with arrows and helices. The secretion tag and residues unable to be built into the electron density are in gray italics. Catalytically important residues are bold and colored as labeled in (B). The A2 section is in pink, and the disulfide cystines are in red.

See also Figure S3.

(Jansson et al., 2010) and CtxB (MacKenzie et al., 1997; Masserini et al., 1992). While the nature of their GM_1 binding sites appears conserved, CfxB binds to blood group A type 2 antigens (Jansson et al., 2010) while glycan arrays indicate that EcxB does not. Such antigens bind the B subunit of the heat-labile toxin using an alternate binding site on the circumferential edge of the pentamer (Holmner et al., 2007). Most residues making up this novel antigen site in LT-IB are conserved across both CfxB and EcxB, including a tyrosine and threonine thought to be important for recognition; further work is needed to confirm differences in blood antigen specificity across the cholera-group B subunits that will aid an analysis of the determinants for this secondary ligand site.

The Unique A Subunit—EcxA

The EcxA subunit is a globular protein consisting of nine α helices, one 3_{10} helix, and three antiparallel β sheets containing 12 strands in total (see Figures 1, 2A, and 2C). While EcxA and CtxA share no sequence similarity, there remained the possibility that they could share structural homology. This was not the case; however, a structure-based search of the Protein Data Bank (PDB) using "Fold" (Krissinel and Henrick, 2004) identified the closest known homolog being that of an inactive form of human pro matrix metalloprotein 2 (Protein Data Bank [PDB] ID, 1EAK; rmsd of 2.1 Å over 116 of 282 C_α, 19 of the 116 residues are conserved). The degree of structural conservation is low, and EcxA could equally well be described as having homology to the catalytic cores of a number of metzincin proteases. Indeed, the majority of conservation between EcxA and MMP2 exists within their respective zinc-binding motifs (residues HExGHxxGxxH; Figure 2 and Figure S3). Despite low sequence similarity between EcxA and MMP-2, the catalytic sections of the fold are largely conserved, implying that EcxA is indeed a metzincin protease (Figure 2). This is not without precedent; an unrelated serine protease makes up the enzymatic A subunit of the subtilase cytoxin AB_5 family (Paton et al., 2004).

The structural core of EcxA resembles that of other metzincin-type metalloproteases. This fold is described as consisting of an upper subdomain prior to the consensus motif and a lower C-terminal subdomain following it (Tallant et al., 2010); this rough division results in the subdomains lying on either side of the peptide-binding cleft overlaying the active-site helix (h6 in EcxA). In EcxA, this classical metzincin fold division is confused, as N-terminal residues form an integral part of the C-terminal subdomain structure. The lower subdomain of EcxA could be described as the base sitting atop the B subunits; this consists of one of the β sheets (s1, s10, s11, s12, s2), a backing helix (h8), an N-terminal helix (h1), and several long loops (elements shown as partially transparent in Figure 2A). The upper subdomain of EcxA, like other metzincins, contains most of the catalytic machinery: the active-site helix provides two of three zinc-coordinating histidines ($H^{179}EIGH^{183}$) and the proposed catalytic base Glu-180 (Figure 2). The third metal-coordinating histidine, His-189, arises from the loop immediately C terminal to helix 6. Electron density provides clear evidence for a metal ion coordinated by these three histidines in EcxA (greater than 10 σ peaks in omit and anomalous difference Fourier maps). This ion is modeled as zinc due to a peak in X-ray fluorescence scans and homology

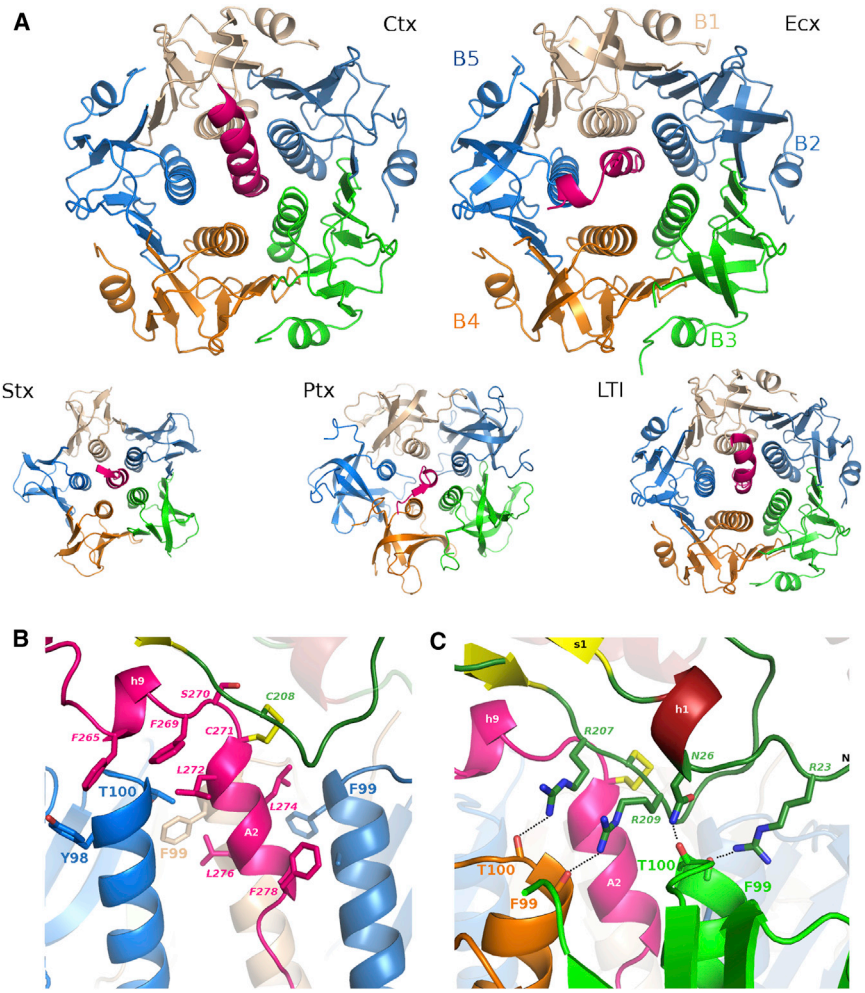

Figure 3. Interactions Making Up the EcxA-B Interface

(A) Top: overview of the B subunit pentameric structure with inserted A2 helices shown for the cholera toxin (Ctx) and Ecx. Bottom: smaller scale views in the same orientation for Shiga toxin (Stx), pertussis toxin (Ptx), and the *E. coli* heat-labile endotoxin I (LTI). Coloring is as in Figure 2A.

(B) The hydrophobic intersubunit interaction interface showing the EcxA helix 9 and helix A2 in pink. EcxA residues are labeled with italic font, and EcxB residues are labeled with standard roman font according to the color of their originating subunit. The Cys-208-Cys-271 redox switch disulfide is shown at the top.

(C) The hydrogen bonds EcxA makes to $EcxB_3$ and B_4 via its N-terminal residues and s11 loop are shown.

See also Figure S2.

with the catalytic sites of other metzincins. The ion has a distorted square pyramidal coordination to the three-histidine's epsilon nitrogens and two water molecules. Matrix metalloproteinase metzincins frequently bind other metal ions via their acidic S loop, an area of the protease involved in substrate recognition. In contrast, EcxA possesses only its catalytic zinc ion, having a more abridged loop at this site (see Figures 2A and 2B), and no further unmodeled peaks are observed in the electron density. An absence of noncatalytic metal ions in EcxA is one of several features conserved among MMPs missing in this protein. On the basis that flexible regions of the protein may confuse structural searches, we expanded our comparison of the EcxA metzincin fold to encompass a broader range of such proteases.

The metzincin clan of metalloproteases is found in all domains of life. It is described in terms of lineages of closely related proteins including the MMPs, astacins, serralysins, adamalysins/ADAMs/reprolysins, snapalysins, leishmanolysins, pappalysins (Gomis-Rüth, 2009), and the more recently characterized fragilysins, archaemetzincins, and cholerilysins. Distinguishing features of metzincin endopeptidases include a methionine-containing turn required for the structural integrity of the catalytic zinc-binding site and the subsequent substrate-binding loop (Tallant et al., 2010). In MMPs, this Met turn is directly C terminal to helix 6 (see Figure 2B). EcxA, instead, has a large loop inserted at this point that delves toward the B pentamer, with β strands s10 and s11 extending the lower subdomain's β sheet before returning 29 residues later to form a Met turn. The returning s11 loop is important as it contains Cys-208, which participates in the A subunit's only disulfide bond. AB_5 toxins frequently contain a redox-sensing disulfide whose reduction inside the host cell acts as a switch to promote subunit dissociation and A subunit activation. As discussed later, in Ecx, this disulfide is in an unusual position directly above the B subunits' pentameric pore. When compared with other metzincins, EcxA thus contains structural elements inserted within its catalytic machinery that extend to interface with the toxin B subunits. The intact nonreduced EcxAB holotoxin showed no proteolytic activity in a nonspecific small scale test (see Figure S4D). Active metzincins have a hydrophobic cavity adjacent to the catalytic zinc ion. A large aromatic residue within the substrate inserts into the cavity, π-stacking with a metal-coordinating histidine while forming backbone and side chain interactions with a conserved tyrosine within the substrate loop. In the EcxAB structure, the substrate loop of EcxA does not adopt an active conformation; what should be a hydrophobic pocket next to the zinc ion is instead large and polar. The missing pocket is due to the conformation of the EcxA substrate-binding loop; although a tyrosine is present, instead of forming one wall of the hydrophobic pocket, it is oriented away from the active site and toward the B pentamer (see Tyr-224 and pink substrate loop in Figure 2A). The B-subunit-bound form of EcxA may thus represent that of a proenzyme, the correct folding of the A subunit's catalytic machinery potentially requiring its dissociation from the pentameric ring following cellular delivery.

Table 2. Glycan Array Analysis of EcxB

Glycan No.	Structure	Mean Relative Fluorescence Units	Coefficient of Variation (%)
141	Galβ1-3GalNAcβ1-4(Neu5Acα2-3)Galβ1-4Glcβ-Sp0[a] (GM_1)	7,112	12
63	Fucα1-2Galβ1-3GalNAcβ1-4(Neu5Acα2-3)Galβ1-4Glcβ-Sp9[a] (Fucosyl-GM_1)	2,954	6
62	Fucα1-2Galβ1-3GalNAcβ1-4(Neu5Acα2-3)Galβ1-4Glcβ-Sp0 (Fucosyl-GM_1)	1,798	30
297	Galβ1-3Galβ1-4GlcNAcβ-Sp8[a]	707	6
139	Galβ1-3GalNAcβ-Sp8	231	67
231	Neu5Acα2-3(Neu5Acα2-3Galβ1-3GalNAcβ1-4)Galβ1-4Glcβ-Sp0	214	42

Data are presented for a selection of 6 of the 511 glycans present on the array; a histogram plot of the entire array is presented in Figure S4E. Complete data sets are available at http://www.functionalglycomics.or/glycomics/publicdata/selectedScreens.jsp. Data are for quadruplicate array spots.
[a]Sp0, Sp8, and Sp9 designate $CH_2CH_2NH_2$, $CH_2CH_2CH_2NH_2$, and CH_2 $CH_2CH_2CH_2CH_2NH_2$ linkers, respectively.

EcxA, Prototype for a Toxilysin Metzincin Family

Proteins within each metzincin family share similar ancillary additions to their core metalloprotease fold arising out of conserved family-specific sequences (Gomis-Rüth, 2009). One such characteristic region occurs within the loop spanning between the zinc-binding HExGHxxGxxH motif and the subsequent conserved methionine turn, residues important for enzymatic activity and substrate specificity (Gomis-Rüth, 2003). The sequence of this region shows considerable homology among family members to the point of "family-specific" residue positions being defined C terminal to the third histidine and two residues N terminal to the methionine turn. The remainder of the zinc-binding/Met-turn sequence is also used to help identify members of a particular metzincin family, even if they otherwise have low homology outside this region. This loop within EcxA (residues 179–218; Figure 2C) is elongated through insertion of the s10, s11 β strands and did not immediately resemble previously defined metzincin family sequences (Gomis-Rüth, 2009). We thus compared the structure of EcxA to metzincins from each major family. This was done with particular focus on metzincins with large loops within their zinc-binding/Met-turn sequence including the astacins, serralysins, pappalysins, cholerilysins, and leishmanolysins but also the snapalysins because of their single conserved cysteine within this loop (Gomis-Rüth, 2009). The structure of the EcxA zinc-binding/Met-turn loop diverges from that observed in other metzincins; it is part of the B-pentamer-interacting loop that contains half of the AB_5 redox switch and extends the lower subdomain's β sheet, a pentamer-interacting β sheet that is one of several features marking the EcxA metzincin fold as significantly different from previously observed structures. Other aspects include the insertion of two short helices (h4 and h5) N terminal to the active-site helix that also line one end of the EcxA substrate cleft and a two-stranded s4 s5 β sheet wrapping around the back of the molecule (see Figure 2A). A lack of sequence conservation and the sheer disparity between the EcxA structure and previously solved metzincins, as well as its exclusive association as part of a heterohexameric AB_5 toxin, would attest that this protein stands as a prototype for a family of metzincin proteases, a family that we propose to call the toxilysins. This metzincin family includes EcxA and CfxA-type proteins (e.g., BAC16523, WP_016231354, WP_001575760, and BAC16521) and, potentially, a number of other related proteins that are yet to be fully characterized. We are working to define the characteristic sequence determinants and substrate specificity for the family but would expect the zinc-binding/Met-turn sequence to resemble H-E-x-x-H-x-x-G-x-x-H-N-[~16]-C-[~6]-P-S/A-I/L-M. The potential length of this loop, the necessity of the conserved asparagine, and the position of the redox-switch cysteine are all aspects, for some variability in other family members could be expected. It will next be important to characterize the substrates, activation mechanism, and sequence determinants of the toxilysin family of proteases.

The Ecx Oligomerization Interface

The B subunits of the AB_5 toxins oligomerize to form stable pentameric rings that bind to their respective A subunits. The OB folds of the toxins' B subunit are well conserved, their oligomerization yielding a central pore ~15 Å in diameter symmetrically lined with five copies of the residues from one face of the B subunits' longest h2 helix. One of the stabilizing features of the mature holotoxins is the insertion of the A subunit's C-terminal A2 helix directly into the central pore of the pentamer. The residues lining the pore vary in different proteins, but the two ends can generally be ascribed distinct characteristics (see Figure S2); the end directly interfacing with the A subunit is frequently hydrophobic, presenting a cylindrical interaction surface for the respective toxin's A2 helix (Tinker et al., 2003). In contrast, the membrane-proximal side of the channel is more often charged or polar in character.

The A2 helices of different AB_5 toxin families are unrelated. They vary in overall length and angle of approach to the pore (Figure 3), but the segment contained within the pentameric ring is globally similar. An archetypical toxin C terminus enclosed by its B subunit ring would be described as consisting of a centrally aligned A2 α helix exactly matched in size to the hydrophobic half of the pore that then transitions into a looser strand-like structure, with a smaller diameter, that may be poorly defined at the pore's membrane-proximal end (see Figure 5). The A2 segment of Ecx is unorthodox for two reasons: first, the A subunits activating intramolecular disulfide resides immediately above the pore, with Cys-271 being the N-capping residue of a short A2 helix (see Figure 3B); second, instead of forming an α helix at the center of the pore, it is the first toxin to contain an off-center 3_{10} helix that does not completely fill the space provided (see Figure 3A).

An average α helix is 12 Å in diameter including side chains; this provides an almost perfect match to the diameter of the B subunit's pentameric pore. The off-center orientation and

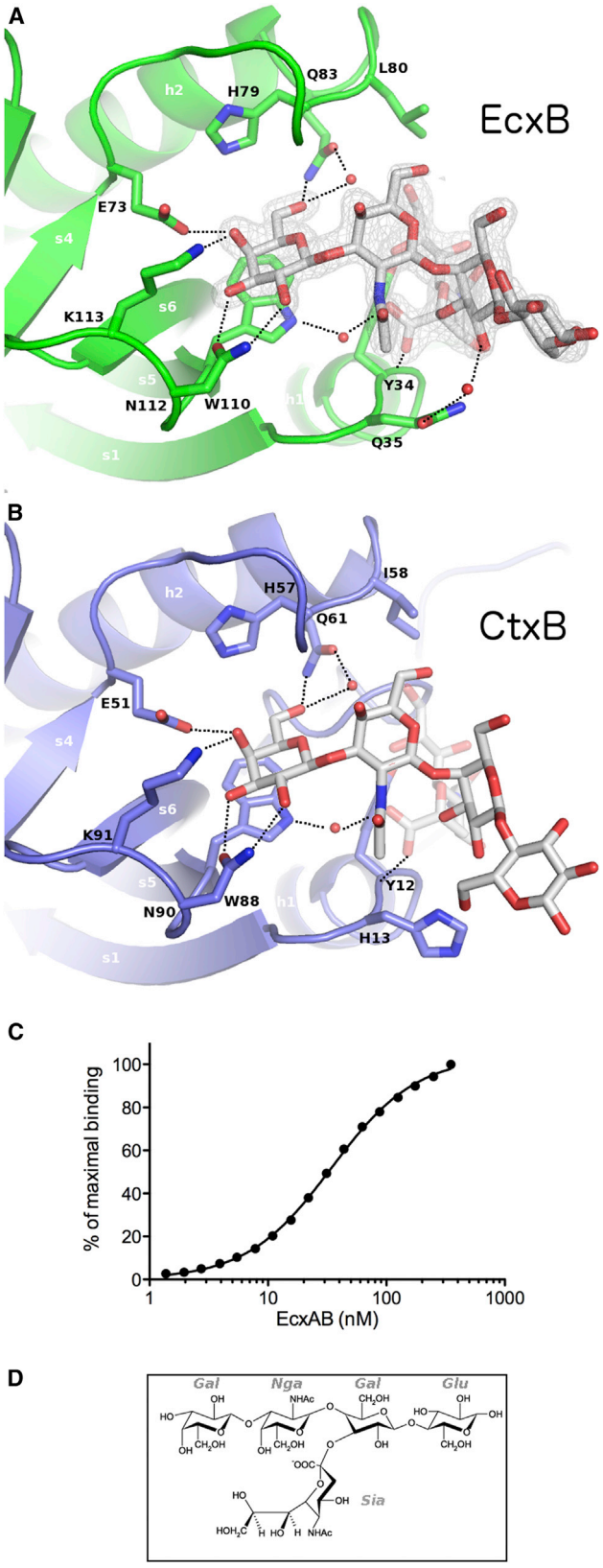

Figure 4. The GM1 Binding Site in Ecx and Ctx

(A) The residues making up the GM_1 binding site of the EcxB subunit are presented ($EcxB_3$ molecule shown). Black dotted lines represent hydrogen bond interactions made between the protein and GM_1. Components of the s2 s3 loop from the adjacent monomer provide additional van der Waals contacts but are excluded for the sake of clarity. The composite OMIT map contoured at 1.5 σ displays the representative density into which GM_1 was built.

(B) For comparison, the equivalent orientation of the previously solved GM_1 binding site within the cholera toxin (Merritt et al., 1997) and the chemical structure of GM_1 are shown.

(C) Percentage of maximal response obtained from the surface plasmon resonance binding curves for EcxAB binding to GM_1. Data represent two independent experiments performed in duplicate. Error is represented as SEM.

(D) For reference, the chemical structure of GM_1.

See also Figure S4 and 3D Molecular Model S2.

smaller diameter of the Ecx A2 helix result in its making drastically different interactions with the different EcxB subunits. The A2 helix itself is eight residues long and alternates between large hydrophobic residues on one side and small glycine or alanine residues on the other. Inside the pore, the large hydrophobic leucine and phenylalanine residues pack against the three Phe-99 side chains of subunits $EcxB_1$, B_2, and B_5 (see Figure 3B). The EcxA:EcxB complex is stabilized further by polar contacts to the C termini of helix 2 in $EcxB_5$, B_3, and B_4 (see Figures 3B and 3C). The charged hydrogen bonds made by Arg-207 and Arg-209 with the backbone of $EcxB_4$ are particularly interesting, as Cys-208 is the other half of the activating disulfide. Thus, the two cystines of the EcxA intramolecular disulfide are located next to major elements of the EcxA:EcxB interface: the A2 helix for Cys-271 and the s11 arginine loop for Cys-208. AB_5 toxins usually contain an A1-A2 linking intramolecular disulfide that is reduced following internalization, resulting in dissociation of the A subunit and its activation. The integral nature of the disulfide within the EcxAB intersubunit interface makes it easy to see how its reduction could promote such dissociation. Moreover, as the s11 arginine loop lies beneath the catalytic zinc ion of EcxA within the zinc-motif/Met turn loop, this could also provide a means by which dissociation could affect activation of the peptidase.

EcxB and CtxB show 63% sequence identity and almost complete structural homology, yet their A subunits are distinct. How is it possible for a common B subunit usage to exist in the cholera and Ecx families of toxins? Prior to the structure of Ecx, the sequence homology of AB_5 toxins indicated that they existed as closely matched pairs, coevolving a highly stable interaction mechanism. There are only three residue differences between EcxB and CtxB within their respective A subunit binding sites. Despite this, the two pentamers carry completely unrelated cargo proteins attached through divergent A2 interaction mechanisms. The three substitutions in EcxB/CfxB correspond to Gly-101, Phe-99, and Ala-96 (respectively, Glu-79, Leu-77, and Ile-74 in Ctx; see Figure S1). These residues are all part of the hydrophobic mouth of the pentameric pore, and mutational studies have proven their equivalents to be important for A subunit binding in CtxB (Tinker et al., 2003). Apart from its A2 helix, the intersubunit interactions of EcxA are mostly made with backbone groups of EcxB (see Figure 3B). Providing that pentaradiate symmetry is maintained, many residue changes could thus potentially be tolerated within the B subunit using an A2 3_{10} helix interface. The presence of Ala-96 in EcxB instead of the CtxB

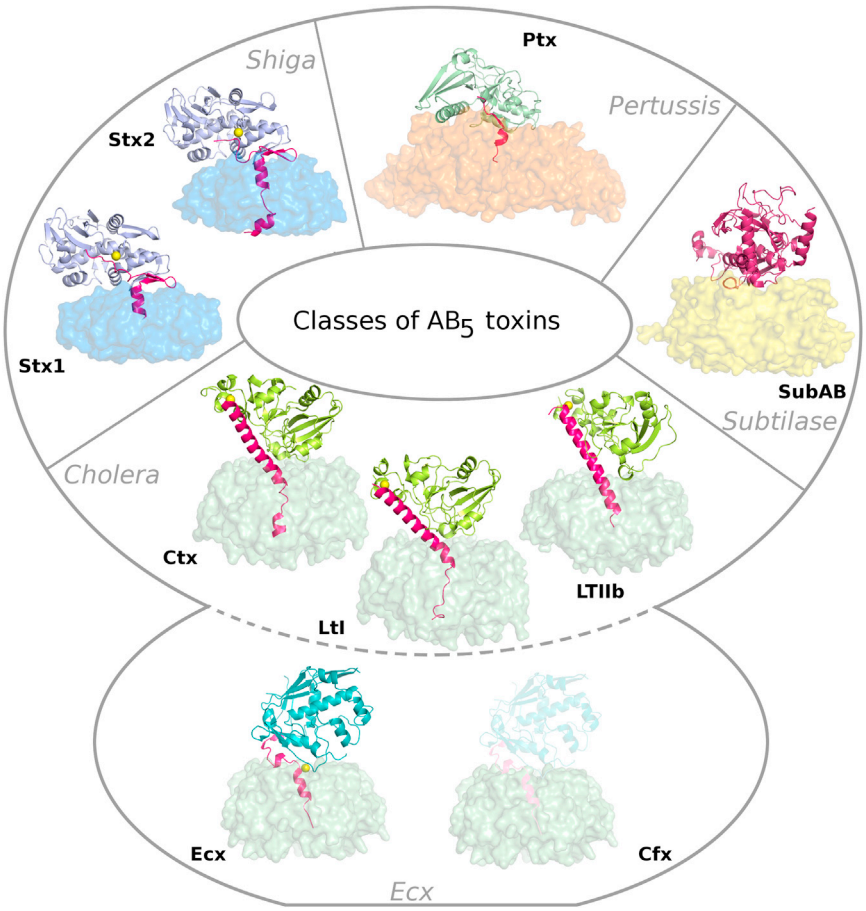

Figure 5. Organization of the AB_5 Toxin Classes

Four AB_5 toxin classes have been defined via shared sequence relationships in both their A and B subunits. The structures of known AB_5 holotoxins divided into their respective classes are displayed using the same colors for subunits with sequence homology. The pentameric B subunit is shown using a partially transparent surface representation. The A subunits with cartoon representations in which the A2 domain is highlighted in pink are shown. The activating disulfide is shown using a yellow dot.

isoleucine would seem necessary to allow for the off-center binding mode of the 3_{10} helix. However, the converse does not appear to be true, as LT-IIb binds its A2 helix with an Ala in this position. Chimeric AB_5 toxins prove that residue changes in the A2 region can alter holotoxin stability and may be all that lies between the potency differences of cholera and heat-labile enterotoxins (Rodighiero et al., 1999). The structure of EcxAB suggests that such intersubunit interactions with the B subunits of AB_5 proteins are more permissive and less fine-tuned than previously thought.

Cytotoxic Activity of EcxAB

Cytotoxicity of the EcxAB protein was examined in several cell lines, of which the most sensitive were Chinese hamster ovary (CHO) cells. Treatment of subconfluent CHO monolayers with 5 μg/ml EcxAB holotoxin induced a pronounced cell rounding effect after 24 hr incubation. This effect was dependent on the presence of the enzymatic A subunit, as no cytopathic effect was seen when cells were treated with a similar concentration of EcxB (Figure 6). Cytopathic effects were not seen in Vero (African green monkey kidney) cells treated with EcxAB (data not shown). Differential susceptibilities of cell lines to distinct AB_5 toxins is commonplace. For example, Vero cells are highly susceptible to both SubAB and Stx (50% cytotoxic doses in the picogram range for both toxins), whereas CHO cells are susceptible to SubAB but refractory to Stx (Paton et al., 2004). This is attributable, at least in part, to differences in expression of the distinct cognate glycan receptors (α2-3-linked *N*-glycolylneuraminic acid glycans and the glycolipid globotriaosyl ceramide for SubAB and Stx, respectively) (Byres et al., 2008; Paton and Paton, 1998). Clearly, levels of expression of GM_1 on the surface of target cells would be expected to influence susceptibility to EcxAB, possibly accounting for low potency. However, whether a cytotoxic phenotype is visible at the microscopic level in a given cultured cell line is also dependent on the physiological consequences of A-subunit-mediated covalent modification of its target molecule. Whereas Stx and SubAB cause lethal damage in Vero cells, other AB_5 toxins may have more subtle effects. Ctx, for example, is bound and internalized by Vero cells, confirming display of the cognate receptor GM_1 (Chong et al., 2008), but it exerts no obvious cytopathic phenotype in this cell line. The culture supernatants of bacterial isolates expressing Ecx/Cfx also show low cytotoxicity in suckling mouse and CHO cell assays (Karasawa et al., 2002). Thus, the Ecx family may be relatively low potency toxins. Further work is ongoing to identify the substrate(s) of EcxAB and to characterize its mechanism of action and its transport following cellular uptake.

Conclusions

It is somewhat a dichotomy that the different AB_5 toxin classes have structurally related B subunits while their respective A subunit cargos radically diverge. This has led to the hypothesis that the B subunits evolved into an efficient cellular delivery and internalization system that became independently partnered with a variety of toxic A subunits (Beddoe et al., 2010). The A subunits of the different toxin classes may have convergently evolved unrelated connection systems utilizing C-terminal A2 helices and redox-switch release mechanisms, because this is a highly effective way for a protein to be transported into a host, sense their surroundings, and then dissociate. The EcxAB holotoxin structure presented here provides a prototype for a family of AB_5 toxins, one that is a partial hybrid with the cholera family and fits this evolutionary hypothesis well. The Ecx/Cfx family of

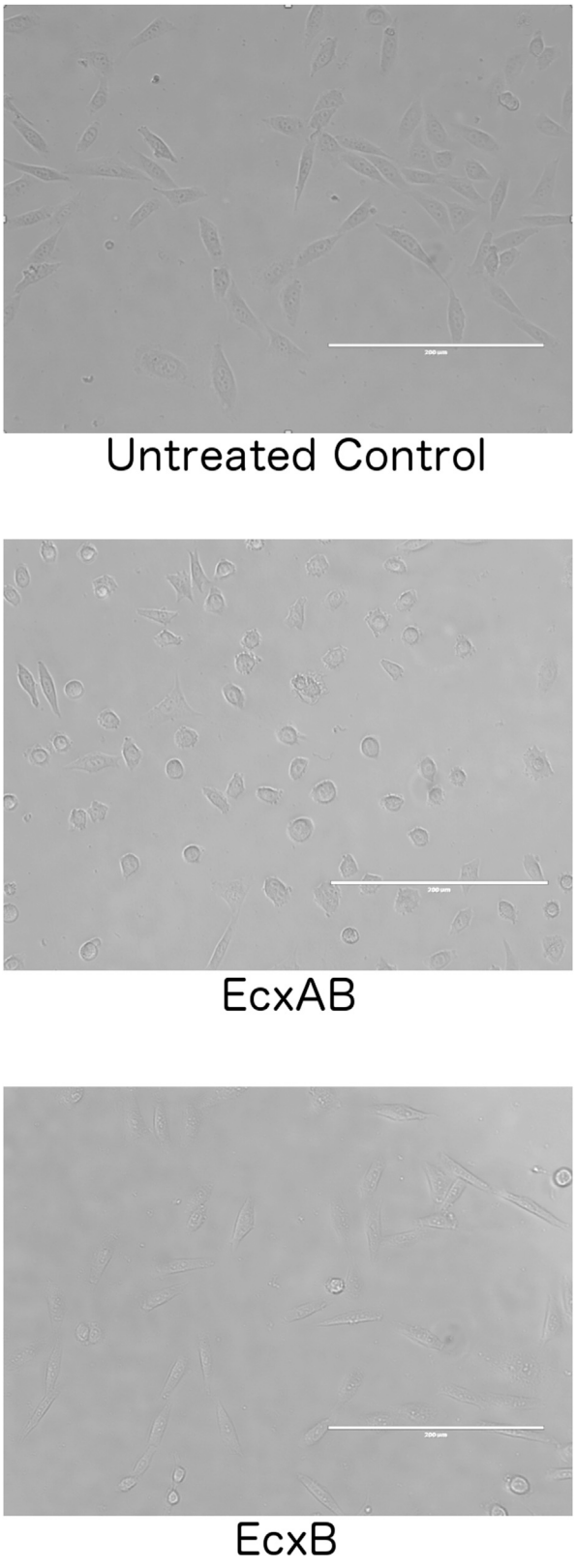

Figure 6. Cytotoxicity of EcxAB for CHO Cells
Subconfluent CHO cells were treated with or without 5 μg/ml EcxAB or EcxB for 24 hr and then examined microscopically. Scale bar, 200 μm.

toxins is found in at least two bacterial species (Karasawa et al., 2002) and could be present in many more. EcxB shares 63% sequence identity to CtxB, and, structurally, the two proteins overlay almost perfectly, indicating close evolutionary links. This is in juxtaposition to EcxA, which is not an ADP-ribosyltransferase like previous cholera family toxins but rather is a novel metalloprotease. Moreover, EcxA has a unique A2-interacting domain comprising a redox-switch-linked 3_{10} helix immediately above the pentamer pore. The novel nature of the metzincin-type metallopeptidase domain of EcxA and its B subunit-binding mechanism can only mean that Ecx and Ctx toxins have independently evolved their pairing to an ancestral cholera family B subunit with minimal divergence since this time. Ecx toxin presents a model for AB_5 toxins that will force us to adapt our current family definitions if drastically different toxin A subunits can bind to almost identical B subunits. This remarkable ability of AB_5 proteins to recruit new toxic payloads is demonstrated in an even more ad hoc manner in the case of the Typhoid toxin (Song et al., 2013); this toxin consists of a *Pertussis*-like AB_5 heterohexamer but one in which a second catalytic subunit is added on to the first pentamer-inserting A subunit through the evolution of a novel intermolecular disulfide crosslink.

The isolated B subunit structure of the *C. freundii* CfxAB is homologous to that of EcxB (Jansson et al., 2010). However, while Jansson et al. characterized the specificity of CfxB, they were unclear whether they had correctly identified the CfxA subunit, as its A2 domain shared no homology with Ctx or LT-I. The sequence identity between CfxA and EcxA allows us to conclude that not only is it a toxilysin metallopeptidase, but also that it would bind to its B subunit utilizing an A2 3_{10} helix. Experiments are being performed to determine any posttranscriptional steps required for activation of this family of AB_5 toxin metalloproteases and which host proteins are their substrates. The Ecx toxin family was identified from bacterial isolates of patients with clinical diarrhea due to its B subunit's relationship to CtxB (Karasawa et al., 2002). Despite this, the enzymatic A subunit normally thought of as responsible for disease causation is not conserved. This raises some unusual questions: Does EcxA induce secretory diarrhea by increasing Cl^- efflux through an independent cellular pathway? If so, why would Ecx and Ctx, two distinct toxins identified by linked disease pathology, share a common B subunit cargo carrier? Is this a case of multiple bacterial strains occupying common environmental niches leading to horizontal gene transfer, and, if so, how rapid is this process?

Rates of cholera infection are greatly reduced following immune stimulation by the inactivated whole cell/recombinant B subunit vaccine. This vaccine is targeted toward *V. cholerae* infection yet also provides a measure of protection against enterotoxigenic *E. coli* due to homology between the two toxins' B subunits (Torrell et al., 2009). The vaccine's makeup may be even more fortuitous if cholera-like B subunits are found in clinically relevant pathogens utilizing AB_5 toxins with distinct catalytic domains.

EXPERIMENTAL PROCEDURES

Cloning, Expression, and Purification of a Soluble Form of EcxAB

Detailed methods used for the cloning, overexpression, purification, and crystallization of soluble EcxAB have been published previously (Ng et al., 2013).

Briefly, EcxA and EcxB were cloned for periplasmic coexpression within *E. coli* B21(DE3) then purified by a combination of immobilized metal affinity and size exclusion chromatography.

Cloning, Expression, and Purification of a Refolded Form of EcxAB

Two gene constructs for EcxA and EcxB, containing their respective native signal sequence, were synthesized by GenScript. The EcxA construct contained *Nco*I and *Not*I restriction sites at the N and C termini, respectively, with these sites used to subclone from the pUC57 cloning vector into the MCS1 of the pETDuet-1 expression vector (Novagen). The EcxB construct contained *Nde*I and *Xho*I restriction sites at the N and C termini, respectively, with these sites used to subclone from the pUC57 cloning vector into the MCS2 of the pETDuet-1 expression vector.

The EcxA- and EcxB-encoding plamids were transformed into *E. coli* BL21(DE3) cells following sequence verification, and EcxA and EcxB were expressed in an insoluble form as inclusion bodies. The cells were grown in Luria broth containing 100 μg/ml ampicillin to an optical density 600 of 0.6. BL21(DE3) cells were induced by the addition of 1.5 mM isopropyl-β-D-1-thiogalactopyranoside for 4 hr. Cell culture pellet was collected following centrifugation at 5000 × *g* for 20 min at 4°C, resuspended in Tris-buffered saline, and stored at −20°C. The cell pellet was thawed, lysed using a cell disruptor (Avestin), and centrifuged at 30,000 × *g* for 30 min at 4°C. Inclusion bodies were washed twice with 50 mM Tris-HCl, pH 8, 100 mM NaCl, 1 mM β-mercaptoethanol, 0.2 mM phenylmethanesulfonylfluoride (PMSF), 0.5% Triton X-100, and then washed once with 50 mM Tris-HCl, pH 8, 1 mM β-mercaptoethanol, 0.2 mM PMSF. Following washing, the inclusion bodies were dissolved in 20 ml resolubilization buffer containing 6 M guanidine hydrochloride, 100 mM Tris-HCl, pH 8, 5 mM β-mercaptoethanol. The solubilized pellet was slowly diluted into 2 l refold buffer containing 50 mM Tris-HCl, pH 8, 500 mM NaCl, 5 mM imidazole and stirred overnight at room temperature. Purification of the refolded form of EcxAB is as described for the soluble form.

Cytotoxicity Assay

Cytotoxocity assays were performed using CHO and Vero cells, as described elsewhere (Paton et al., 2004).

Crystallization and Data Analysis

Apo Form of EcxAB

Crystals were grown using the hanging-drop, vapor-diffusion method, with a 1:1 (v/v) ratio of EcxAB to mother liquor (well volume, 1 ml). Appearance of crystals from the soluble form of EcxAB occurred within 3 days in 4% tacsimate, pH 4.5, 10% polyethylene glycol 3350. Crystals were flash-frozen in liquid nitrogen before data collection with 20% glycerol as the cryoprotectant.

EcxAB with GM1 Pentasaccharide Bound

Crystals were grown using the hanging-drop, vapor-diffusion method, with a 1:1 (v/v) ratio of EcxAB to mother liquor (well volume, 1 ml). Appearance of crystals from the refolded form of EcxAB occurred within 3 days in 0.8 M NaH_2PO_4, 0.8 M KH_2PO_4, 0.1 M HEPES Na, pH 7.5. GM1 pentasaccharide (Enzo Life Sciences) was added so that the final concentration was approximately 10 mM in drops containing preformed crystals. GM1 was allowed to soak into these crystals for 3 days before flash-freezing in liquid nitrogen and subsequent data collection, using 2 M CH_3CO_2K as the cryoprotectant.

Structure Determination

All diffraction data were collected at 100K on beamline MX2 of the Australian synchrotron. Diffraction data from crystals of the apo- and GM1-soaked EcxAB were obtained at 1.86 Å and 1.80 Å, respectively. The crystals belong to the spacegroup $P6_522$ and contain one molecule in the asymmetric unit. The structure of apo EcxAB was obtained using a single chain of CtxB (Merritt et al., 1997) (PDB ID 2CHB) as a molecular replacement model in the program PHASER (McCoy, 2007; McCoy et al., 2007). As no close homolog of the A subunit was initially identified, ARP/wARP (Langer et al., 2008; Murshudov et al., 2011) was used to build a starting model for the A subunit. A largely complete holotoxin structure resulted, followed by rounds of manual building and refinement. Model building and structural validation were completed using the CCP4 suite (Winn et al., 2011), PHENIX (Adams et al., 2010), and Coot (Emsley et al., 2010). Solvent molecules were retained only if they had acceptable hydrogen bonding geometry contacts of 2.5 Å–3.5 Å with protein atoms or with existing solvent and were in good $2F_o - F_c$ electron density. The final holotoxin model consists of residues 22–126 from five EcxB molecules, residues 21–67, 72–102, and 108–282 from EcxA and a Zinc ion. The GM1-soaked structure was obtained using the apo EcxAB as a molecular replacement model; electron density was clear for all sugar moieties of all five GM1 molecules. A summary of data collection and refinement statistics is provided in Table 1.

Glycan Array Analysis

Purified EcxAB protein at 0.2 μg/ml was applied to a glycan microarray slide at the CFG Protein-Glycan Interaction Core at Emory University. Binding was detected using fluorescence-conjugated anti-hexahistidine antibody. The data are reported as average relative fluorescence units of four of six replicates (after removal of the highest and lowest values) for each glycan represented on the array.

SPR Analysis

All SPR experiments were conducted at 25°C on a BIAcore 3000 instrument using HEPES-buffered saline (10 mM HEPES-HCl, pH 7.4, 500 mM NaCl, and 0.005% P20 [v/v]). Biotinylated synthetic carbohydrates utilized in the SPR studies were obtained either from the CFG Glycan Array Synthesis Core or GlycoTech. The biotinylated glycans—$CH_2CH_2NH_2$-biotin (Sp0), Galβ(1-4)-Glcα-Sp0-biotin, GM1-Sp0-biotin, and αNeu5Ac-Sp0-biotin—were immobilized on an SA-Chip (GE Healthcare) with a surface density of approximately 200 response units. Various concentrations of EcxAB (1.17 to 350 nM) were injected over the captured glycans at 10 μl/min. The surface was regenerated with two injections of 4 M $MgCl_2$ at 100 μl/min between injections of EcxAB. The final response was calculated by subtracting the response of the blank flow cell alone (Sp0) from the EcxAB-glycan complex. The equilibrium data were analyzed using GraphPad Prism.

ACCESSION NUMBERS

The atomic coordinates and observed structure factors have been deposited in the Research Collaboratory for Structural Bioinformatics PDB with codes 4L63 and 4L6T.

SUPPLEMENTAL INFORMATION

Supplemental Information includes four figures, a detailed description of the GM1 binding site, and two 3D molecular model files and can be found with this article online at http://dx.doi.org/10.1016/j.str.2013.08.024.

ACKNOWLEDGMENTS

This research was undertaken on the MX1 and MX2 beamlines at the Australian Synchrotron. The authors acknowledge the CFG, funded by the National Institute of General Medical Sciences grants GM62116 and GM98791, for services provided by the Glycan Array Synthesis Core (The Scripps Research Institute), which produced the mammalian glycan microarray and the Protein-Glycan Interaction Core (Emory University School of Medicine) that assisted with analysis of samples on the array. We thank the staff of the Monash Macromolecular Crystallisation facility. This work was supported by Program and Project grants from the National Health and Medical Research Council of Australia (NHMRC) and Discovery grants from the Australian Research Council. T.B. is a Pfizer Australian Research Fellow; A.W.P. is an Australian Research Council Discovery Outstanding Researcher Award Fellow; J.C.P. is an NHMRC Senior Principal Research Fellow; and J.R. is an NHMRC Fellow.

Received: July 22, 2013
Revised: August 29, 2013
Accepted: August 30, 2013
Published: October 3, 2013

REFERENCES

Adams, P.D., Afonine, P.V., Bunkóczi, G., Chen, V.B., Davis, I.W., Echols, N., Headd, J.J., Hung, L.W., Kapral, G.J., Grosse-Kunstleve, R.W., et al. (2010).

PHENIX: a comprehensive Python-based system for macromolecular structure solution. Acta Crystallogr. D Biol. Crystallogr. *66*, 213–221.

Beddoe, T., Paton, A.W., Le Nours, J., Rossjohn, J., and Paton, J.C. (2010). Structure, biological functions and applications of the AB5 toxins. Trends Biochem. Sci. *35*, 411–418.

Byres, E., Paton, A.W., Paton, J.C., Löfling, J.C., Smith, D.F., Wilce, M.C., Talbot, U.M., Chong, D.C., Yu, H., Huang, S., et al. (2008). Incorporation of a non-human glycan mediates human susceptibility to a bacterial toxin. Nature *456*, 648–652.

Chong, D.C., Paton, J.C., Thorpe, C.M., and Paton, A.W. (2008). Clathrin-dependent trafficking of subtilase cytotoxin, a novel AB5 toxin that targets the endoplasmic reticulum chaperone BiP. Cell. Microbiol. *10*, 795–806.

De Haan, L., and Hirst, T.R. (2004). Cholera toxin: a paradigm for multi-functional engagement of cellular mechanisms (Review). Mol. Membr. Biol. *21*, 77–92.

Emsley, P., Lohkamp, B., Scott, W.G., and Cowtan, K. (2010). Features and development of Coot. Acta Crystallogr. D Biol. Crystallogr. *66*, 486–501.

Fraser, M.E., Chernaia, M.M., Kozlov, Y.V., and James, M.N. (1994). Crystal structure of the holotoxin from Shigella dysenteriae at 2.5 A resolution. Nat. Struct. Biol. *1*, 59–64.

Gomis-Rüth, F.X. (2003). Structural aspects of the metzincin clan of metalloendopeptidases. Mol. Biotechnol. *24*, 157–202.

Gomis-Rüth, F.X. (2009). Catalytic domain architecture of metzincin metalloproteases. J. Biol. Chem. *284*, 15353–15357.

Holmner, A., Askarieh, G., Okvist, M., and Krengel, U. (2007). Blood group antigen recognition by Escherichia coli heat-labile enterotoxin. J. Mol. Biol. *371*, 754–764.

Holmner, A., Mackenzie, A., Okvist, M., Jansson, L., Lebens, M., Teneberg, S., and Krengel, U. (2011). Crystal structures exploring the origins of the broader specificity of escherichia coli heat-labile enterotoxin compared to cholera toxin. J. Mol. Biol. *406*, 387–402.

Jansson, L., Angström, J., Lebens, M., Imberty, A., Varrot, A., and Teneberg, S. (2010). Carbohydrate binding specificities and crystal structure of the cholera toxin-like B-subunit from Citrobacter freundii. Biochimie *92*, 482–490.

Karasawa, T., Ito, H., Tsukamoto, T., Yamasaki, S., Kurazono, H., Faruque, S.M., Nair, G.B., Nishibuchi, M., and Takeda, Y. (2002). Cloning and characterization of genes encoding homologues of the B subunit of cholera toxin and the Escherichia coli heat-labile enterotoxin from clinical isolates of Citrobacter freundii and E. coli. Infect. Immun. *70*, 7153–7155.

Krissinel, E., and Henrick, K. (2004). Secondary-structure matching (SSM), a new tool for fast protein structure alignment in three dimensions. Acta Crystallogr. D Biol. Crystallogr. *60*, 2256–2268.

Langer, G., Cohen, S.X., Lamzin, V.S., and Perrakis, A. (2008). Automated macromolecular model building for X-ray crystallography using ARP/wARP version 7. Nat. Protoc. *3*, 1171–1179.

MacKenzie, C.R., Hirama, T., Lee, K.K., Altman, E., and Young, N.M. (1997). Quantitative analysis of bacterial toxin affinity and specificity for glycolipid receptors by surface plasmon resonance. J. Biol. Chem. *272*, 5533–5538.

Masserini, M., Freire, E., Palestini, P., Calappi, E., and Tettamanti, G. (1992). Fuc-GM1 ganglioside mimics the receptor function of GM1 for cholera toxin. Biochemistry *31*, 2422–2426.

McCoy, A.J. (2007). Solving structures of protein complexes by molecular replacement with Phaser. Acta Crystallogr. D Biol. Crystallogr. *63*, 32–41.

McCoy, A.J., Grosse-Kunstleve, R.W., Adams, P.D., Winn, M.D., Storoni, L.C., and Read, R.J. (2007). Phaser crystallographic software. J. Appl. Crystallogr. *40*, 658–674.

Merritt, E.A., and Hol, W.G. (1995). AB5 toxins. Curr. Opin. Struct. Biol. *5*, 165–171.

Merritt, E.A., Sarfaty, S., Pizza, M., Domenighini, M., Rappuoli, R., and Hol, W.G. (1995). Mutation of a buried residue causes loss of activity but no conformational change in the heat-labile enterotoxin of Escherichia coli. Nat. Struct. Biol. *2*, 269–272.

Merritt, E.A., Sarfaty, S., Jobling, M.G., Chang, T., Holmes, R.K., Hirst, T.R., and Hol, W.G. (1997). Structural studies of receptor binding by cholera toxin mutants. Protein Sci. *6*, 1516–1528.

Murshudov, G.N., Skubák, P., Lebedev, A.A., Pannu, N.S., Steiner, R.A., Nicholls, R.A., Winn, M.D., Long, F., and Vagin, A.A. (2011). REFMAC5 for the refinement of macromolecular crystal structures. Acta Crystallogr. D Biol. Crystallogr. *67*, 355–367.

Ng, N., Littler, D., Le Nours, J., Paton, A.W., Paton, J.C., Rossjohn, J., and Beddoe, T. (2013). Cloning, expression, purification and preliminary X-ray diffraction studies of a novel AB5 toxin. Acta Crystallogr. Sect. F Struct. Biol. Cryst. Commun. *69*, 912–915.

Paton, A.W., and Paton, J.C. (1998). Detection and characterization of Shiga toxigenic Escherichia coli by using multiplex PCR assays for stx1, stx2, eaeA, enterohemorrhagic E. coli hlyA, rfbO111, and rfbO157. J. Clin. Microbiol. *36*, 598–602.

Paton, A.W., Srimanote, P., Talbot, U.M., Wang, H., and Paton, J.C. (2004). A new family of potent AB(5) cytotoxins produced by Shiga toxigenic Escherichia coli. J. Exp. Med. *200*, 35–46.

Rodighiero, C., Aman, A.T., Kenny, M.J., Moss, J., Lencer, W.I., and Hirst, T.R. (1999). Structural basis for the differential toxicity of cholera toxin and Escherichia coli heat-labile enterotoxin. Construction of hybrid toxins identifies the A2-domain as the determinant of differential toxicity. J. Biol. Chem. *274*, 3962–3969.

Song, J., Gao, X., and Galán, J.E. (2013). Structure and function of the Salmonella Typhi chimaeric A(2)B(5) typhoid toxin. Nature *499*, 350–354.

Stein, P.E., Boodhoo, A., Armstrong, G.D., Cockle, S.A., Klein, M.H., and Read, R.J. (1994). The crystal structure of pertussis toxin. Structure *2*, 45–57.

Tallant, C., Marrero, A., and Gomis-Rüth, F.X. (2010). Matrix metalloproteinases: fold and function of their catalytic domains. Biochim. Biophys. Acta *1803*, 20–28.

Tinker, J.K., Erbe, J.L., Hol, W.G., and Holmes, R.K. (2003). Cholera holotoxin assembly requires a hydrophobic domain at the A-B5 interface: mutational analysis and development of an in vitro assembly system. Infect. Immun. *71*, 4093–4101.

Torrell, J.M., Aumatell, C.M., Ramos, S.M., Mestre, L.G., and Salas, C.M. (2009). Reduction of travellers' diarrhoea by WC/rBS oral cholera vaccine in young, high-risk travellers. Vaccine *27*, 4074–4077.

van den Akker, F., Sarfaty, S., Twiddy, E.M., Connell, T.D., Holmes, R.K., and Hol, W.G. (1996). Crystal structure of a new heat-labile enterotoxin, LT-IIb. Structure *4*, 665–678.

Winn, M.D., Ballard, C.C., Cowtan, K.D., Dodson, E.J., Emsley, P., Evans, P.R., Keegan, R.M., Krissinel, E.B., Leslie, A.G., McCoy, A., et al. (2011). Overview of the CCP4 suite and current developments. Acta Crystallogr. D Biol. Crystallogr. *67*, 235–242.